RC 21605 (log 97421) 19 November 99 **Materials Science**

Research Report

Bottom Electrode Effects in Controlling Orientation of Lead Zirconate Titanate Films Deposited by Chemical Solution Deposition

Deborah A. Neumayer, Katherine L. Saenger, Robert B. Laibowitz,
Thomas M. Shaw, Rebecca Mih, Alfred Grill

IBM T. J. Watson Research Center
P. O. Box 218
Yorktown Heights, NY 10598

BOTTOM ELECTRODE EFFECTS IN CONTROLLING ORIENTATION OF LEAD ZIRCONATE TITANATE FILMS DEPOSITED BY CHEMICAL SOLUTION DEPOSITION

DEBORAH A. NEUMAYER, KATHERINE L. SAENGER, ROBERT B. LAIBOWITZ,
THOMAS M. SHAW, REBECCA MIH, ALFRED GRILL
IBM, T.J. Watson Research Center, P.O. Box 218, Yorktown Heights, NY 10598

ABSTRACT

The microstructure and electrical properties of lead zirconate titanate $Pb(Zr,Ti)O_3$ (PZT) films prepared by chemical solution deposition (CSD) with and without lead titanate (PT) seed layers were examined as a function of Ir/Ir oxide electrode type. The novel PZT CSD solution was prepared from a mixture of zirconium and titanium butoxyethoxides and lead ethylhexanoate dissolved in butoxyethanol. The use of excess-lead ($Pb_{xs}Ti$) and stoichiometric PT seed layers was found to promote PZT(111) orientation on Ir but not on Ir oxide. Ir substrate thickness was observed to influence orientation of PZT deposited on stoichiometric PT with greater PZT(111) texturing on thinner Ir(111) substrates. PZT with greater PZT(111) texturing tended to have greater remanent polarization (2Pr, $\mu C/cm^2$). PZT deposited on stoichiometric PT seed layers on Ir(111) was of higher film quality than PZT deposited on $Pb_{xs}Ti$ seed layers on Ir(111). The PZT films deposited on stoichiometric PT on Ir(111) had enhanced PZT(111) orientation, a reduced pyrochlore content, and tended to saturate at lower coercive fields, have higher remanent polarization, squarer hysteresis loops with less tilt and greater fatigue endurance. The use of iridium oxide top electrode was demonstrated to significantly improve fatigue endurance compared to use of an iridium top electrode.

INTRODUCTION

Because of its high remanent polarization and relatively low processing temperature, PZT is a prime candidate for use as ferroelectric in a nonvolatile random access memory (NVRAM). However, because of the poor fatigue endurance of Pt/PZT/Pt ferroelectric capacitors, development of an alternative capacitor structure with alternative electrode materials, such as iridium/iridium oxide, is necessary [1]. Proper control of PZT orientation through electrode selection and use of seed layers to control PZT nucleation can lead to enhanced 2Pr and improved fatigue endurance. Lead titanate seed layers have been demonstrated to influence the orientation of PZT deposited on Pt by chemical vapor deposition [2], sputtering [3], and chemical solution deposition (CSD) [4,5]. In this study we looked at the influence of lead titanate seed layers on PZT deposited by CSD on iridium and iridium oxide electrodes.

EXPERIMENTAL

Chemical Solution Deposition of PZT

The CSD solutions were prepared from a mixture of zirconium and titanium butoxyethoxides and lead ethylhexanoate dissolved in butoxyethanol [6]. The films were deposited by spin casting on Ir and Ir oxide bottom electrodes sputter deposited at 250 °C on SiO_2/Si substrates. Before spinning PZT, two parts PZT CSD solution (0.73M, $Pb_{1.1}Zr_{.4}Ti_{.6}$) were diluted with one part butoxyethanol. The spinning solution was loaded into a syringe and 0.45 and 0.1 μm syringe filters were attached. The solution was syringed on the substrate until completely wetted. The substrate was then spun for 50 sec at 2500 rpm. After each spin-coating, the samples were baked on a hot plate at 150 °C for 1-3 min, then at 350 °C for 3-10 minutes in air. The PT seed layers were prepared by diluting one part stoichiometric PT CSD solution (0.64M, Pb_1Ti_1) or $Pb_{xs}Ti$ (0.62M, $Pb_{1.3}Ti_1$) with 9 parts butoxyethanol before spin casting. The PT seed layers were annealed at 700 °C for 1s in oxygen using an AG-Associates Model 410 rapid thermal annealer (RTA). Three layers of PZT were deposited, then rapidly thermally annealed in O_2 at 700 °C for 5 sec, followed by a furnace anneal at 650 °C for 60 min.

PZT Film Characterization

X-ray diffraction (XRD) spectra were obtained using a Philips PW1729 diffractometer with Cu Kα radiation. Hysteresis loops were measured with either a Radiant Technology RT66A ferroelectric test system or a standard Sawyer-Tower circuit. Capacitor top electrodes were fabricated by sputtering of iridium and iridium oxide through a shadow mask at room temperature. After top electrode deposition, a RTA post electrode anneal at 650 °C for 10 min. in flowing oxygen was conducted before electrical measurements.

RESULTS

PZT deposited on iridium oxide without a PT seed layer was observed to have a random orientation, regardless of PZT stoichiometry or thickness. PZT deposited on iridium oxide with lead titanate seed layers also had a random orientation, regardless of seed layer stoichiometry, thickness, and PZT composition and thickness. Thin PZT films, typically 100 nm or less, deposited on Ir(111) without a PT seed layer were observed to be preferentially PZT(100) oriented. Thicker PZT films, typically 150 nm or more, deposited on Ir(111) without a PT seed layer were observed to be randomly oriented. A similar dependence of PZT orientation on thickness was observed for PZT deposited on Pt /Ti substrates without seed layers.

Lead titanate seed layers were observed to influence PZT orientation on Ir(111) substrates. As shown in Fig.1a, PZT (109/47/45) spun without a PT seed layer was randomly oriented. PZT deposited on a ~1 nm thick $Pb_{xs}Ti$ seed layer, spun from 1:100 dilution, was randomly oriented (Fig. 1b). PZT deposited on a ~5 nm thick $Pb_{xs}Ti$ seed layer, spun from 1:20 dilution was preferentially PZT(100) oriented as evidenced by an enhancement of the PZT(100) peak intensity (Fig. 1c). PZT deposited on a ~10 nm thick, $Pb_{xs}Ti$ seed layer spun from 1:10 dilution, was preferentially PZT(111) textured as evidenced by the increase in the PZT(111) peak intensity and suppression of the PZT(100) peak intensity (Fig. 1d). Oxidation of the underlying Ir substrate is observed in the XRD after anneal of seed layer and after PZT anneal (Fig. 1a). The enhancement of the PZT(111) with a $Pb_{xs}Ti$ seed layer from a 1:10 dilution was observed to be reproducible and independent of the overlying PZT composition in PZT films up to 300 nm thick. As shown in Fig. 2, three layer ~300 nm thick PZT with Pb/Zr/Ti compositions: 109/49/42 (Fig. 2a), 104/54/43 (Fig. 2c), 108/71/31 (Fig. 2e) spun on a PT (1:10 dilution) seed layer was preferentially PZT(111) oriented. However, if the overlying PZT layer was too thick, the PT seed layer effect was suppressed. As shown in Fig. 2, the six layer films (~600 nm, Figs. 2b,d,f) are preferentially PZT(100) textured.

Use of a stoichiometric PT seed layer resulted in a marked improvement in PZT film quality including enhanced PZT(111) orientation, reduced PZT(100) peak intensity and a reduced pyrochlore content, relative to PZT deposited on $Pb_{xs}Ti$ seed layer (Fig. 3). The excess lead in $Pb_{xs}Ti$ seed layer seed layer seemed to inhibit PZT(111) texturing and crystallization resulting in a two phase pyrochlore/pervoskite structure (Fig. 3b). A similar effect of excess lead inhibiting PZT(111) texturing and enhancing PZT(100) texturing was observed for PZT deposited on Pt without seed layers . The enhancement of the PZT(111) orientation with a stoichiometric PT seed layer is reproducible (see results listed in Table 1) and was observed to be independent of PZT stoichiometry.

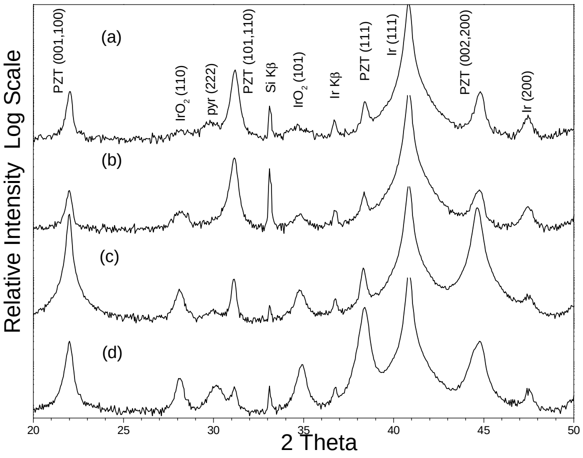

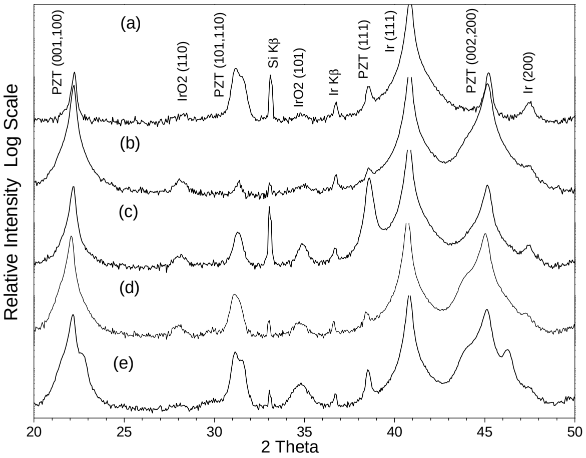

Figure 1 (left): (θ,2θ) XRD spectra of 180 nm PZT(109/47/45)/Ir/SiO_2/Si (a) without a PT seed layer. (b-e) PZT/PT/Ir/SiO_2/Si with a $Pb_{xs}Ti$ seed layer spun from a (b) 1:100 dilution, (c) 1:20 dilution, (d) 1:10 dilution.

Figure 2 (right): (θ,2θ) XRD spectra of PZT/Ir/SiO_2/Si with a $Pb_{xs}Ti$ seed layer spun from a 1:10 dilution, (a,c,f) 3L PZT, (b,d,f) 6L PZT (a,b) 109/49/42, (c,d) 104/54/43, (e,f) 108/71/31 PZT composition.

As summarized in Table 1, a correlation was observed between the thickness of the Ir substrate and the peak intensity ratio of the PZT(111) and PZT(100) reflections, I(111)/I(100), of PZT spun on stoichiometric PT seed layer. A larger PZT I(111)/I(100) ratio was observed on thinner Ir substrates. The enhanced PZT(111) texturing on stoichiometric PT seed layers on thin Ir(111) may be related to grain size, roughening, stress, or degree of oxidation of the underlying Ir(111) substrate or competition between oxidation of the Ir and crystallization of the PZT.

Table 1: Summary of XRD reflection intensities of PZT spun on stoichiometric PT seed layer on Ir/IrO_2/SiO_2/Si substrates.

Ir (nm)	IrO_2 (nm)	PZT (nm)	I(111)/I(100)	I(100)	I(110)	I(111)
10	100	220	30	990	880	28,000
20	0	220	30	930	670	26,000
20	50	230	25	1,040	940	25,000
20	100	220	13	1,800	950	23,000
50	100	220	15	1,900	900	26,800
100	100	220	10	1,700	680	17,200
200	50	260	7	1,300	1,400	9,400

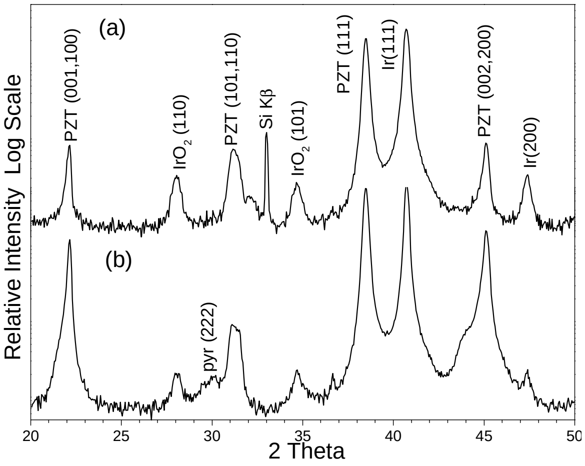

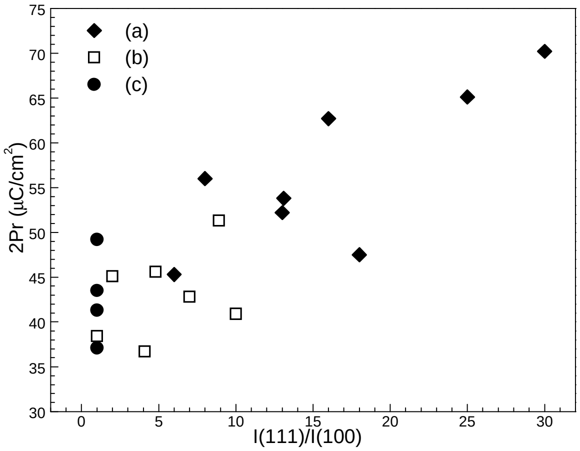

Figure 3 (left): $(\theta, 2\theta)$ XRD spectra of PZT/Ir/SiO_2/Si with a PT seed layer spun from a 1:10 dilution, (a) stoichiometric PT seed layer, (b) $Pb_{xs}Ti$ seed layer.
Figure 4 (right): Remanent polarization at 4V plotted relative to XRD peak intensity ratio I(111)/I(100) for furnace annealed PZT films deposited on (a,b) Ir(111) with (a) stoichiometric PT seed layer, (b) $Pb_{xs}Ti$ seed layer, (c) iridium oxide with iridium top electrodes.

We observed a correlation between XRD peak intensity ratio I(111)/I(100) and 2Pr. PZT films deposited on stoichiometric PT tend to have larger I(111)/I(100) ratios and correspondingly greater 2Pr values (Fig. 4a) than comparable PZT films grown on $Pb_{xs}Ti$ seed layers (Fig. 4b). PZT films grown on Ir oxide have random orientation with 2Pr comparable to PZT films grown on $Pb_{xs}Ti$ seed layers (Fig. 4c). We observed that randomly oriented PZT films spun without a seed layer have lower 2Pr than comparable PZT films spun on PT seed layers. We also observed that PZT films which were not furnace annealed at 650 °C for 60 min had lower 2Pr despite having similar I(111)/I(100) ratios to comparable furnace annealed PZT films. The lower 2Pr associated with non-furnace annealed films may be related to PZT grain size effect.

PZT films spun on stoichiometric PT seed layers have larger I(111)/I(100) ratios and tend to saturate at lower coercive fields, have higher remanent polarization, squarer hysteresis loops with less tilt, and greater fatigue endurance relative to PZT spun on $Pb_{xs}Ti$ seed layer. As shown in Fig. 5, PZT films spun on $Pb_{xs}Ti$ seed layer with Ir top and bottom electrodes have poor fatigue endurance; after 10^4 cycles the hysteresis loop is shifted and nearly collapsed with a nearly 80% loss of polarization. In contrast, PZT films spun on stoichiometric PT experienced little shift of the hysteresis loops and retained 30% polarization after 10^{11} cycles (Fig. 6). The poorer electrical properties of PZT spun on $Pb_{xs}Ti$ seed layers may be related to the reduced PZT(111) orientation, the two phase pyrochlore/pervoskite structure observed in the XRD or possibly to an accumulation of excess PbOx in the grain boundaries. The greater fatigue endurance of PZT spun on stoichiometric PT seed layers supports S.H. Kim et al. hypothesis that the initial seed layer has an accumulation of negatively charged lead vacancies and the overlying PZT film has an accumulation of positively charged oxygen vacancies which become associated near the seed layer and main film interface. The resultant associated vacancies have lower mobility and can act as a barrier to accumulation of oxygen vacancies near the film/electrode interface resulting in improved fatigue [4]. Fatigue endurance of PZT spun on stoichiometric PT was significantly improved with the use of an iridium oxide top electrode. As shown in Fig. 7, PZT spun on stoichiometric PT retained 80% polarization after 10^{11} cycles and experienced no shift in the hysteresis loop. A direct comparison of the improved fatigue is shown in Fig. 8.

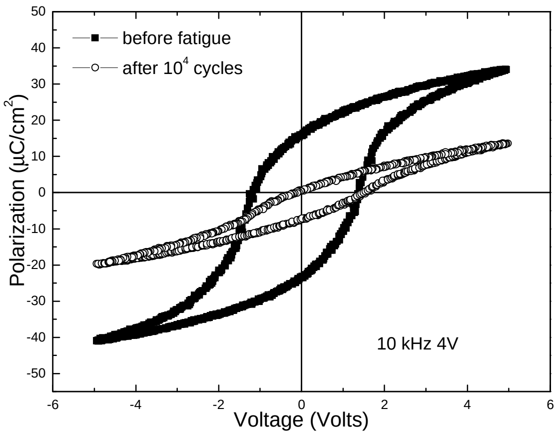

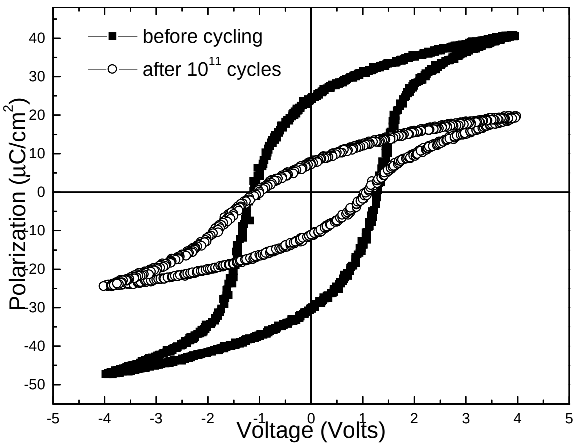

Figure 5 (left): Fatigue hysteresis loops measured at 4V, 10 kHz of Ir/PZT/Ir/SiO_2/Si with a $Pb_{xs}Ti$ seed layer spun from a 1:10 dilution and Ir 100 nm top electrode measured before fatigue and after 10^4 cycles at 4V, 10 kHz.

Figure 6 (right): Fatigue hysteresis loops measured at 4V, 1 MHz of Ir/PZT/Ir/SiO_2/Si with a stoichiometric lead titanate seed layer spun from a 1:10 dilution and Ir 100 nm top electrode measured before fatigue and after 10^{11} cycles at 4V, 10 kHz.

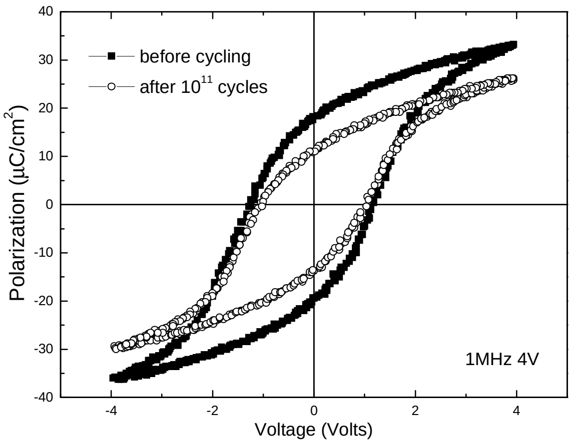

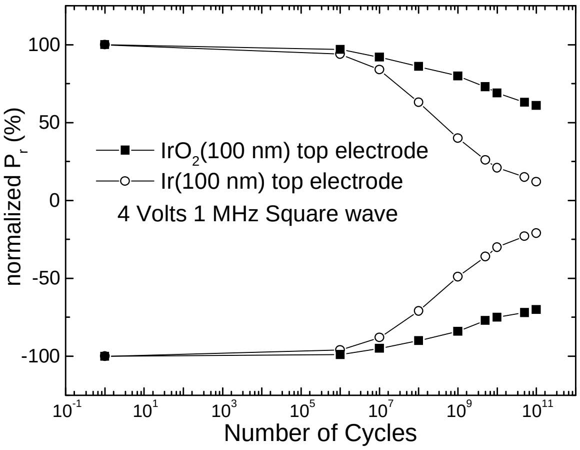

Figure 7 (left): Fatigue hysteresis loops measured at 4V, 1 MHz of IrO_2/PZT/Ir/SiO_2/Si with a stoichiometric lead titanate seed layer spun from a 1:10 dilution measured and iridium oxide top electrode before fatigue and after 10^{11} cycles at 4V, 10 kHz.

Figure 8 (right): Comparison of fatigue measured at 4V, 1 MHz of Iridium and Ir oxide top electrodes on PZT/Ir/SiO_2/Si with a stoichiometric lead titanate seed layer spun from a 1:10 dilution.

CONCLUSIONS

The use of $Pb_{xs}Ti$ and stoichiometric PT seed layers was found to promote PZT(111) orientation on iridium but not on iridium oxide. Ir substrate thickness was observed to influence orientation of PZT deposited on stoichiometric PT with greater PZT(111) texturing on thinner Ir(111) substrates. A correlation was observed that films with larger I(111)/I(100) ratios tend to have larger 2Pr. PZT deposited on stoichiometric PT seed layer on Ir(111) was of higher film quality than PZT deposited on $Pb_{xs}Ti$ seed layers. The PZT films deposited on stoichiometric PT on Ir(111) have enhanced PZT(111) orientation, a reduced pyrochlore content, and tend to saturate at lower coercive fields, have higher remanent polarization, squarer hysteresis loops with less tilt and greater fatigue endurance. The use of iridium oxide top electrode was demonstrated to significantly improve fatigue endurance compared to use of an iridium top electrode

ACKNOWLEDGEMENTS

The authors would like to acknowledge Roy Carruthers for deposition of iridium and iridium oxide top electrodes.

REFERENCES

1. N. Izumi, Y. Fujimori, T. Nakamura, A. Kamisawa, IEICE Trans. Electron., **E81-C**, p.513 (1999).
2. M. Shimizu, M. Sugiyama, H. Fujisawa, T. Hamano, T. Shiosaki, K. Matsushige, J. Cryst. Growth, **145**, p. 226 (1994).
3. N.-H. Cho, H.-G. Kim, Microelec. Eng., **29**, p. 243 (1995).
4. S.-H. Kim, D.-J. Kim, S.K. Streiffer and A.I. Kingon, **14**, p. 2476, 14 (1999).
5. C.K. Kwok, S.B. Desu, J. Mater. Res., **8**, p.339 (1993).
6. D.A. Neumayer, P.R. Duncombe, U.S. Patent No. 5 962 654 (5 October 1999).
7. K. Aoki, Y. Fukuda, A. Nishimura, Jpn. J. Appl. Phys., **9B**, P.4147 (1993).
8. T. Atsuki, N. Soyama, G. Sasaki, T. Yonezawa, K. Ogi, K. Sameshima, K. Hoshiba, Y. Nakao, A. Kamisawa, Jpn. J. Appl. Phys., **9B**, p. 5196 (1994).